MRI对新辅助化疗后乳腺原发肿瘤退缩模式预测的准确度

杨　涛[1,2]，刘雁冰[1]，张朝蓬[1]，刘　广[1]，穆殿斌[1]，王永胜[1]

1.山东省肿瘤医院乳腺病中心，山东 济南 250117；
2.连云港市第一人民医院放疗科，江苏 连云港 222002

［摘要］ **背景与目的：**新辅助化疗(neoadjuvant chemotherapy，NAC)可使原发肿瘤较大的乳腺癌患者获得保乳治疗(breast-conserving therapy，BCT)机会，但NAC后原发肿瘤退缩模式影响保乳率及预后。本研究旨在观察MRI对NAC后乳腺原发肿瘤退缩模式预测的准确度。**方法：**61例ⅡA~ⅢC期乳腺浸润性导管癌患者，NAC后手术标本制作次连续病理大切片，显微镜下勾画残余肿瘤范围，Photoshop软件配准，3D-DOCTOR软件三维重建病理及MRI图像残余肿瘤模型，评价NAC后原发肿瘤的病理退缩模式。将其分为外科pCR(无残留灶)、孤立状、结节状、团块伴散在状和弥散状。结合病理退缩模式，将临床-病理退缩模式分为退缩明显型(distinct shrinkage mode，DSM，相比NAC前原发肿瘤最长径，NAC后残余肿瘤最长径退缩比率≥50%且≤2 cm)和非退缩明显型(non-distinct shrinkage mode，NDSM)。**结果：**MRI和病理的退缩模式呈外科pCR、孤立状、结节状、团块伴散在状和弥散状模式分别为23例、17例、5例、9例、7例和18例、3例、13例、20例、7例(P=0.001)。MRI预测病理退缩模式的准确度、灵敏度和特异度分别为86.2%，65.6%和91.4%。MRI和病理呈DSM比例分别为62.3%和59.0%(κ=0.863，P=0.000)。MRI预测临床-病理退缩模式的准确度、灵敏度和特异度分别为91.0%、64.0%和94.8%，其中预测DSM和NDSM差异均无统计学意义(P均>0.05)。MRI预测临床-病理退缩模式的受试者工作特征(receiver operating characteristic，ROC)曲线下面积为0.928(P=0.000)。**结论：**NAC后MRI三维重建图像能准确模拟并预测残余肿瘤的立体空间位置，有助于选择NAC后降期BCT患者。

［关键词］ 乳腺癌；退缩模式；新辅助化疗；三维重建；MRI

DOI: 10.3969/j.issn.1007-3969.2016.02.009

中图分类号：R737.9　　**文献标志码：**A　　**文章编号：**1007-3639(2016)02-0168-09

Accuracy of MRI for predicting shrinkage modes of primary breast tumor following neoadjuvant chemotherapy with three-dimensional reconstruction technique

YANG Tao[1,2], LIU Yanbing[1], ZHANG Zhaopeng[1], LIU Guang[1], MU Dianbin[1], WANG Yongsheng[1] (1.Breast Cancer Center, Shandong Cancer Hospital, Jinan 250117, Shandong Province, China; 2.Department of Radiotherapy, the First People's Hospital of Lianyungang, Lianyungang 222002, Jiangsu Province, China)

Correspondence to: WANG Yong-sheng E-mail: wangysh2008@aliyun.com

［**Abstract**］ **Background and purpose:** The most clearly recognized benefit of neoadjuvant chemotherapy (NAC) is that it can increase the proportion of patients who can be treated with breast-conserving therapy (BCT). However, the shrinkage modes of the primary breast tumor after NAC have been confirmed as a predictor of BCT rate and prognosis. This study is to evaluate the accuracy of MRI predicting the shrinkage mode of the primary breast tumor after NAC with three-dimensional reconstruction technique. **Methods:** Sixty-one women with pathologically proven solitary invasive ductal carcinoma (ⅡA-ⅢC) were recruited. Breast specimens were prepared with PMSS, and residual tumors were microscopically outlined, scanned and registered by PHOTOSHOP software. The 3D model of residual tumors was reconstructed with 3D-DOCTOR software based on pathology and MRI imaging characteristics to evaluate the shrinkage mode. We devided the pathological shrinkage modes into surgical pCR (no residual tumors), solitary lesions without surrounding lesions, multinodular lesions, solitary lesions with adjacent spotty lesions and diffuse lesions. Further, the clinical-pathological shrinkage modes were divided into 2 categories: distinct shrinkage mode

基金项目：山东省医药卫生科技发展计划项目(2011HD012)；山东省科技发展计划项目(2013YD18030)。
通信作者：王永胜　E-mail：wangysh2008@aliyun.com

(DSM, the longest diameter of the pathological residual tumors was less than 50% and ≤2 cm in comparison with the primary tumor before NAC) and non-distinct shrinkage mode (NDSM, the longest diameter of the pathological residual tumors was more than 50% and/or >2 cm in comparison with the primary tumor before NAC). **Results:** The surgical pCR, solitary lesions without surrounding lesions, multinodular lesions, solitary lesions with adjacent spotty lesions and diffuse lesions were observed in 23, 17, 5, 9, 7 and 18, 3, 13, 20, 7 patients by MRI and pathology, respectively (P=0.001). The accuracy, sensitivity and specificity of MRI for predicting pathological shrinkage modes were 86.2%, 65.6% and 91.4%, respectively. The DSM was observed in 36 (59.0%) patients by pathology, and 38 (62.3%) patients by MRI. Two methods had a high consistency in clinical-pathological shrinkage modes (κ=0.863, P=0.000). The accuracy, sensitivity and specificity of MRI for predicting clinical-pathological shrinkage modes were 91.0%, 64.0% and 94.8%, respectively. There was not a statistic difference in prediction between DSM and NDSM by MRI (P>0.05). Receiver operating characteristic (ROC) curve analysis showed an AUC of 0.928 (P=0.000) for MRI to predict the clinical-pathological shrinkage mode. **Conclusion:** Three-dimensional MRI reconstruction after NAC could simulate and predict spatial location of residual tumors, and can be helpful in selecting patients who received BCT after NAC with tumor downstaging.

［**Key words**］ Breast Cancer; Shrinkage mode; Neoadjuvant chemotherapy; Three-dimensional reconstruction; MRI

对于初始肿瘤较大的可手术乳腺癌患者，新辅助化疗(neoadjuvant chemotherapy，NAC)的主要优点在于可以降低临床分期，使有保乳意愿但不适合保乳治疗(breast-conserving therapy，BCT)的患者获得更多的保乳机会，缩小手术范围，改善患者的生活质量[1-4]。NAC后原发肿瘤退缩成多中心残余肿瘤被证实是BCT后同侧乳房肿瘤复发(ipsilateral breast tumor recurrence，IBTR)的影响因素[5-6]。因此，NAC后原发肿瘤退缩模式的准确评估对于BCT患者的选择至关重要。本研究试图通过NAC后残余肿瘤的病理及MRI三维重建，观察MRI对乳腺癌NAC后原发肿瘤退缩模式预测的准确度。

1 资料和方法

1.1 一般资料

选取山东省肿瘤医院乳腺病中心2010年7月—2013年8月接受6~8个周期NAC的ⅡA~ⅢC期女性乳腺癌患者，共61例，年龄31~70岁(中位年龄49岁)。NAC前后均行MRI检查。入选标准：① NAC前所有肿瘤均经空芯针穿刺活检病理证实为浸润性导管癌；② MRI图像及临床检查示原发孤立肿瘤；③ 美国东部肿瘤协作组(Eastern Cooperative Oncology Group，ECOG)评分为0~1分；④ 主要器官功能正常，且Hb≥90 g/L，WBC≥2.0×10^9/ L，ANC≥1.5×10^9/L，PLT≥100×10^9/L，ALT和AST≤$2.5\times$ULN，血肌酐≤$1.5\times$ULN；⑤ 无明显心功能障碍；⑥ NAC后完全切除残余肿瘤(乳腺癌改良根治术/保乳手术)。排除标准：① 既往接受过新辅助治疗(包括NAC和新辅助内分泌治疗)；② 既往其他恶性肿瘤病史；③ 炎性乳腺癌；④ 妊娠哺乳期妇女；⑤ NAC后病灶评价疾病稳定(stable disease，SD)或疾病进展(progressive disease，PD)；⑥ 正在接受其他临床试验，可能对本研究产生影响的患者。

1.2 新辅助化疗方案

采用AC-P方案者32例(52.5%)，TAC方案者23例(37.7%)，FEC方案者2例(3.3%)，AC-PH方案者2例(3.3%)，TCH方案者1例(1.6%)，TP方案者1例(1.6%)。

1.3 次连续病理大切片制作

1.3.1 乳房切除术后标本

根据NAC前超声引导下美兰标记的原发肿瘤范围，放射状地向外扩大3 cm切除乳腺标本，标本放进-20 ℃冰箱12~24 h。乳腺皮肤表面平行划取数道刀痕，平行注射器针道双色涂抹法标记定位点，乳腺标本放置自制大切片取材台，间隔3 mm，平行Y轴取材，平均切30个层面(图1)。切片标记计数，放入铁夹，防止组织变形。自制病理大切片包埋台对组织切片包埋。Leica Microm TP 1020大组织切片机切片，每个蜡块切片2~3张，切片厚度4~6 μm。HE染色封片(表1)。

表 1 制作步骤

Tab. 1 Processing schedules

A		B	
Fixation (formalin)	24 h	Xylene Ⅰ 60 ℃	15-20 min
	70% 1 h	Xylene Ⅱ 60 ℃	15-20 min
	80% 1 h	Alcohol 100% Ⅰ	3-5 min
	85% 1 h	Alcohol 100% Ⅱ	3-5 min
Dehydration (ethanol)	90% 1 h	Alcohol 95%	3-5 min
	95% 1 h	Alcohol 90%	3-5 min
	100% 1 h	Hematoxylin	5-10 min
	100% 1 h	1% acid alcohol	30 s
	2 h	0.2% ammonia water	30-60 s
Clearing (xylene)	2 h	eosin Y solution	1 min
	2 h	Alcohol 90%	2-3 min
Infiltration (paraffin, 60 ℃)	6 h	Alcohol 95%	2-3 min
	6 h	Alcohol 100% Ⅱ	3-5 min
		Alcohol 100% Ⅰ	3-5 min
		Xylene Ⅲ	5-10 min
		Xylene Ⅳ	5-10 min

A: Fixation, dehydration, clearing and infiltration; B: HE staining

1.3.2 乳腺癌保乳术后标本

根据NAC前超声引导下美兰标记的原发肿瘤范围，术者放射状地外扩1 cm切除腺体标本，平行针道埋线标记点位点。以下步骤如上述乳房切除术后标本制作(图1)。

1.4 病理三维重建

在显微镜下勾画出每张切片残余肿瘤边界及钙化点。将Epson V600扫描仪分辨率设定为360 bpi，扫描勾画切片。Photoshop软件导入勾画的切片，乳房切除标本以皮肤刀痕和染料定位点为基准，保乳术后标本以腺体刀痕和线孔为基准，进行切片配准。配准后的切片导入3D-DOCTOR软件，依据显微镜下勾画的残余肿瘤范围及钙化点，在软件中用不同的颜色标记：红色代表浸润性导管癌，绿色代表导管原位癌，紫色代表钙化灶。选择“Edit/Calibrations”指令，弹出图像校准参数对话框，*X*、*Y*轴输入0.07，*Z*轴输入3，单位为mm。使用“3D Rendering/Surface Rendering/Simple Surface”指令，呈现出NAC后残余肿瘤病理三维模型(图2)。

1.5 MRI三维重建

乳腺MRI检查采用飞利浦3.0 T MRI成像系统。乳腺MRI图像以DICM格式刻录到CD光盘，将其导入3D-DOCTOR软件。勾画每张动态增强图像的乳腺肿瘤范围，选择“3D Rendering/Surface Rendering/Simple Surface”指令，三维重建出NAC前后乳腺MRI三维图像模型(图2)。

图 1 乳腺次连续病理大切片制作

Fig. 1 Breast part-mount sub-serial section processing

A: Modified radical mastectomy specimen (specimen was cut 3 cm away from the markers signed before NAC, and the parallel needles smeared with two colors); B: The self-made platform and the operation; C: BCT specimen (purple arrow and yellow arrow separately represent superior margin and external margin, and red arrow indicates localized sutures for images registration)

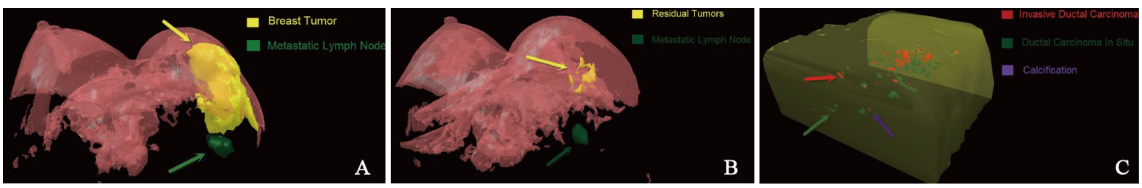

图 2 病理及MRI三维模型

Fig. 2 3D mode of pathology and MRI

A: 3D MRI mode before NAC; B: 3D MRI mode after NAC; C: 3D pathological mode after NAC

1.6 NAC后三维退缩模式

1.6.1 病理退缩模型

① 外科pCR：无残留灶，即乳腺组织所有的浸润性癌和原位癌细胞无残留；② 孤立状：残留孤立肿瘤并周围无散在癌灶；③ 结节状：癌灶呈结节状散在分布，相互无关联；④ 团块伴散在状：孤立团状肿瘤伴散在癌灶；⑤ 弥散状：肿瘤原位消融，呈蜂巢状散在分布(图3)。

1.6.2 临床-病理退缩模型

为了满足NAC后保乳患者的残余肿瘤长径的选择标准，结合病理退缩模式形态，推导出临床-病理退缩模型，分为退缩明显型(distinct shrinkage mode，DSM)和非退缩明显型(non-distinct shrinkage mode，NDSM)。

DSM包括外科pCR、孤立状、结节状和团块伴散在状。以上4种模式满足：相比NAC前原发肿瘤最长径，NAC后残余肿瘤最长径退缩比率≥50%且≤2 cm。

NDSM包括孤立状、结节状、团块伴散在状和弥散状。以上4种退缩模式满足：相比NAC前原发肿瘤最长径，NAC后残余肿瘤最长径退缩比率＜50%和(或)>2 cm。采用MRI测量NAC前原发肿瘤最长径，病理测量NAC后残余肿瘤最长径(图4)。

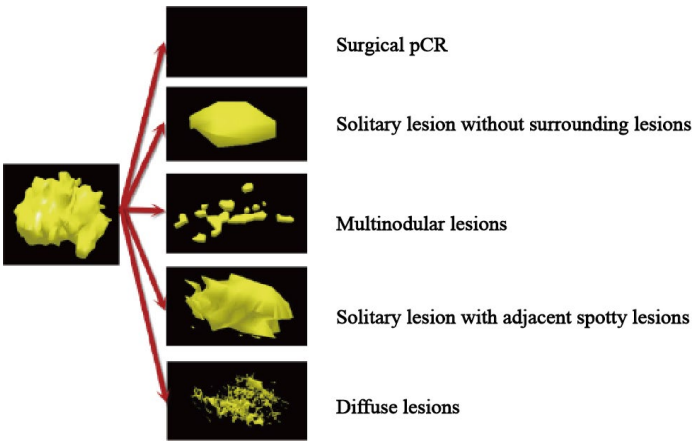

图 3 病理三维退缩模型

Fig. 3 3D pathological shrinkage modes

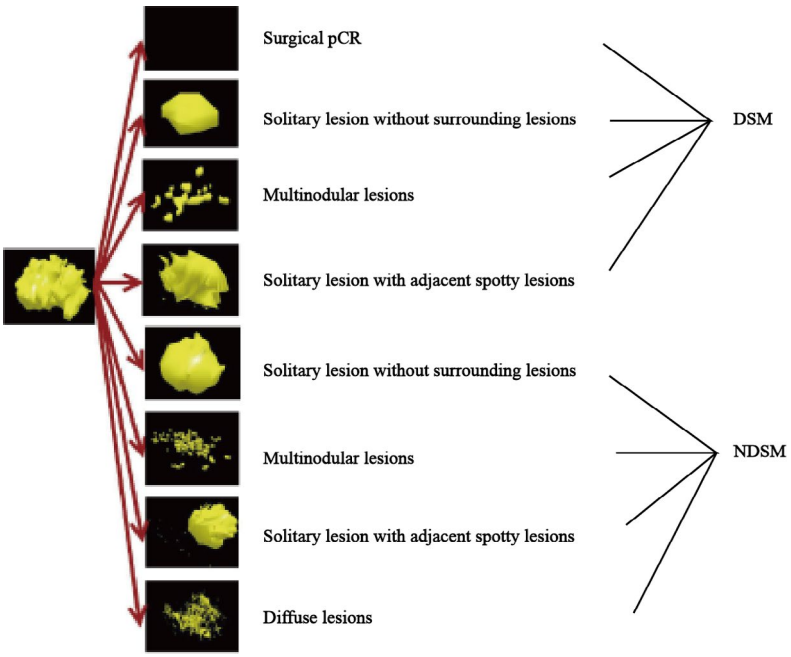

图 4 临床-病理三维退缩模型

Fig. 4 3D clinical-pathological shrinkage modes

1.7 统计学处理

采用SPSS 17.0软件进行数据分析。使用χ^2检验分析率之间的差异。以病理检查为金标准，建立受试者工作特征(receiver operating characteristic，ROC)曲线，计算MRI预测的曲线下面积。P<0.05为差异有统计学意义。

2 结　果

2.1 病理退缩模式

MRI图像退缩模式呈外科pCR、孤立状、结节状、团块伴散在状和弥散状分别为23例(37.7%)、17例(27.9%)、5例(8.2%)、9例(14.8%)和7例(11.5%)，病理检查分别为18例(29.5%)、3例(4.9%)、13例(21.3%)、20例(32.8%)和7例(11.5%)，差异有统计学意义(P=0.006，表2)。MRI预测病理退缩模式的准确度、灵敏度、特异度、阳性预测值和阴性预测值分别为86.2%、65.6%、91.4%、65.6%和91.4%。

MRI预测弥散状模式的准确度与外科pCR相似(P=0.119)，显著优于其他模式(P均<0.05)。预测孤立状模式的特异度和阳性预测值最低(75.9%和17.6%)，均劣于外科pCR、团块伴散在状和弥散状(P均<0.05)。预测外科pCR、孤立状和弥散状模式的阴性预测值最高(100.0%)，显著优于结节状、团块伴散在状(P均<0.05，表3)。

2.2 临床–病理退缩模式

MRI图像呈向心性退缩和非向心性退缩 DSM和NDSM分别为38例(62.3%)和23例(37.7%)；病理检查分别为36例(59.0%)和26例(41.0%)，差异无统计学意义(P=0.854)。两者评价临床–病理退缩模式具有显著的一致性(κ=0.863，P=0.000，表4)。

在MRI评价向心性退缩者DSM中，23例(37.7%)呈外科pCR，10例(16.4%)呈孤立状，2例(3.3%)呈团块伴散在状；在非向心性退缩者NDSM中，6例(9.8%)呈孤立状，3例(4.9%)呈结节状，10例(16.4%)呈团块伴散在状，7例(11.5%)呈弥散状。

在病理检查评价向心性退缩者DSM中，18例(29.5%)呈外科pCR，3例(4.9%)呈孤立状，10例(16.4%)呈结节状，5例(8.2%)呈团块伴散在状；在非向心性退缩者NDSM中，15例(24.6%)呈团块伴散在状，3例(4.9%)呈结节状，7例(11.5%)呈弥散状(表5)。

MRI预测临床–病理退缩模式的准确度、灵敏度、特异度、阳性预测值和阴性预测值分别为91.0%、64.0%、94.8%、64.0%和94.8%。MRI预测向心性退缩和非向心性退缩DSM和NDSM的准确度、灵敏度、特异度、阳性预测值和阴性预测值分别为89.8%、63.9%、94.2%、65.7%、93.8%和92.2%、64.0%、95.4%、61.5%、95.9%，差异无统计学意义(P均>0.05，表6)。MRI预测临床–病理退缩模式的ROC下面积为0.928(95%CI：0.832~0.978，P=0.000，图5)。

表 2　NAC后原发肿瘤的病理与MRI退缩模式

Tab. 2　Shrinkage modes of the primary breast tumor after NAC by pathology and MRI

[*n*(%)]

Shrinkage mode	Pathology	MRI	κ value	P value
Surgical pCR	18(29.5)	23(37.7)		
Solitary lesion without surrounding lesions	3(4.9)	17(27.9)		
Multinodular lesions	13(21.3)	5(8.2)	0.568	0.000
Solitary lesion with adjacent spotty lesions	20(32.8)	9(14.8)		
Diffuse lesions	7(11.5)	7(11.5)		

表 3 MRI预测NAC后原发肿瘤的病理退缩模式

Tab. 3 MRI predicting the pathological shrinkage modes of the primary breast tumor after NAC

Mode	MRI	Pathology		Shrinkage mode/%
		+	-	
Mode Ⅰ	+	18	5	AC=91.8, SE=100.0, SP=88.4, PPV=78.3, NPV=100.0
	-	0	38	
Mode Ⅱ	+	3	14	AC=77.0, SE=100.0, SP=75.9, PPV=17.6, NPV=100.0
	-	0	44	
Mode Ⅲ	+	3	2	AC=80.3, SE=30.0, SP=95.8, PPV=60.0, NPV=82.1
	-	10	46	
Mode Ⅳ	+	9	0	AC=82.0, SE=45.0, SP=100.0, PPV=100.0, NPV=78.8
	-	11	41	
Mode Ⅴ	+	7	0	AC=100.0, SE=100.0, SP=100.0, PPV=100.0, NPV=100.0
	-	0	54	
Total	+	40	21	AC=86.2, SE=65.6, SP=91.4, PPV=65.6, NPV=91.4
	-	21	223	

Mode Ⅰ: Surgical pCR; Mode Ⅱ: Solitary lesion without surrounding lesions; Mode Ⅲ: Multinodular lesions; Mode Ⅳ: Solitary lesion with adjacent spotty lesions; Mode Ⅴ: Diffuse lesions. AC: Accuracy; SE: Sensitivity; SP: Specificity; PPV: Positive predictive value; NPV: Negative predictive value

表 4 NAC后原发肿瘤的临床–病理退缩模式

Tab. 4 Clinical-pathological shrinkage modes of the primary breast tumor after NAC

Shrinkage mode	MRI		Total	κ value	P value
	DSM	NDSM			
Pathology					
DSM	35	1	36	0.863	0.000
NDSM	3	22	25		
Total	38	23	61		

表 5 NAC后原发肿瘤的临床–病理退缩模式的亚组

Tab. 5 The subgroups of clinical-pathological shrinkage modes of the primary breast tumor after NAC

[*n*(%)]

Shrinkage mode	Pathology	MRI
DSM		
Surgical pCR	18(29.5)	23(37.7)
Solitary lesion without surrounding lesions	3(4.9)	10(16.4)
Multinodular lesion	10(16.4)	0(0.0)
Solitary lesion with adjacent spotty lesions	5(8.2)	2(3.3)
NDSM		
Solitary lesion without surrounding lesions	0(0.0)	6(9.8)
Multinodular lesions	3(4.9)	3(4.9)
Solitary lesion with adjacent spotty lesions	15(24.6)	10(16.4)
Diffuse lesions	7(11.5)	7(11.5)

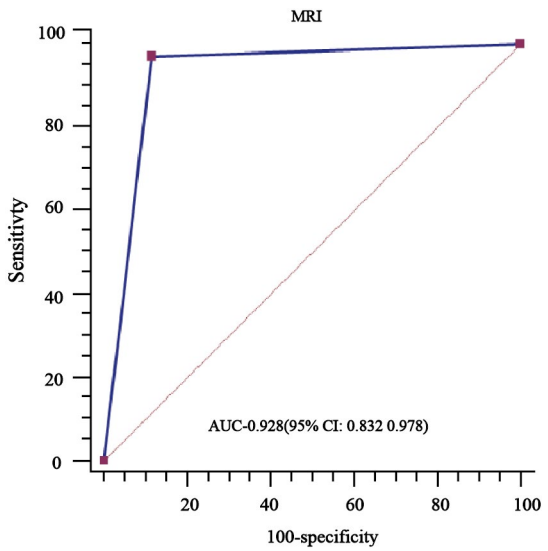

图 5 MRI预测临床–病理退缩模式ROC曲线

Fig. 5 ROC curves of MRI predicting clinical-pathological shrinkage mode

AUC: Area under curve

表 6 MRI预测NAC后原发肿瘤的临床–病理退缩模式

Tab. 6 MRI predicting the clinical-pathological shrinkage modes of the primary breast tumor after NAC

Item	MRI	Pathology		Shrinkage mode/%
		+	-	
DSM				
Mode Ⅰ	+	18	5	AC=91.8, SE=100.0, SP=88.4, PPV=78.3, NPV=100.0
	-	0	38	
Mode Ⅱ	+	3	7	AC=88.5, SE=100.0, SP=87.9, PPV=30, NPV=100.0
	-	0	51	
Mode Ⅲ	+	0	0	AC=83.6, SE=0.0, SP=100.0, PPV=(-), NPV=83.6
	-	10	51	
Mode Ⅳ	+	2	0	AC=91.8, SE=66.7, SP=100.0, PPV=100.0, NPV=94.9
	-	3	56	
Total A	+	23	12	AC=89.8, SE=63.9, SP=94.2, PPV=65.7, NPV=93.8
	-	13	196	
NDSM				
Mode Ⅱ	+	0	6	AC=90.2, SE=(-), SP=90.2, PPV=0.0, NPV=100.0
	-	0	55	
Mode Ⅲ	+	1	2	AC=93.4, SE=33.3, SP=96.6, PPV=16.7, NPV=100.0
	-	2	56	
Mode Ⅳ	+	8	2	AC=85.2, SE=53.3, SP=95.7, PPV=80.0, NPV=86.3
	-	7	44	
Mode Ⅴ	+	7	0	AC=100.0, SE=100.0, SP=100.0, PPV=100.0, NPV=100.0
	-	0	54	
Total B	+	16	10	AC=92.2, SE=64.0, SP=95.4, PPV=61.5, NPV=95.9
	-	9	209	
Total	+	39	22	AC=91.0, SE=64.0, SP=94.8, PPV=64.0, NPV=94.8
	-	22	405	

3 讨 论

NAC可以使部分初始需要乳房切除的患者降期接受BCT，并获得良好的美容效果[1-4]。NAC后行BCT是否会增加后期的IBTR是被普遍关注的问题。NSABP B–18试验[7]中位随访16年，证实NAC后BCT患者的IBTR高于BCT后辅助化疗患者，但差异无统计学意义(P=0.21)。EORTC 10902试验[8]中位随访10年的数据显示，对比初始可行BCT的患者，计划接受乳房切除术的患者NAC后改行保乳手术后的局部复发率并未显著增加，但总生存期更短。Ishitobi等[5]研究发现，NAC后发生IBTR的患者预后更差，且证实了NAC后残余肿瘤呈多中心模式是IBTR的独立影响因素之一。因此，为了成功施行BCT降低IBTR，必须考虑原发肿瘤的范围和肿瘤的退缩模式，并需谨慎检测切缘状况。

目前，MRI已成为NAC后评估残余肿瘤和化疗反应的最佳方法[9-16]。MRI通过对比增强的病灶信号是否降低判断NAC反应，较钼靶和B超能更精确地评估NAC反应，对残余肿瘤范围的评估与病理具有较好的一致性[17]。同时MRI可鉴别残留组织及NAC后引起的纤维增生或坏死组织，有助于帮助选择NAC行保乳手术的患者[16]。但NAC后原发肿瘤退缩的多样性，特别是蜂窝样或散在分布的退缩，降低MRI对NAC后残余肿瘤范围测量的精确性[18]。因此，本研究通过联合NAC后残余肿瘤模型的病理和MRI三维重建，促进残余肿瘤空间关系的可视化，促使MRI更全面、立体、直观地预测NAC后原发肿瘤退缩模式，同时可以提供一项测量肿瘤范围更准确的方法，有助于选择NAC后适合行BCT的患者。

NAC后获得pCR者行BCT后的LRR率较低，且有更好的预后[7]。TBCRC Trial017试验[19]报道，NAC后MRI预测外科pCR的准确度、灵敏度和特异度分别为74.0%、83.0%和47.0%。本研究采用次连续病理大切片技术，提高了残余肿瘤的检出率和MRI预测外科pCR的特异度。另

外，由于化疗药物作用于乳腺组织和血管后破坏了MRI造影剂的传导通路，可能提高了MRI预测外科pCR的灵敏度。Wasser等[20]研究证实，NAC后原发肿瘤无反应者，MRI预测病理的残余肿瘤范围准确度高。同样，本研究证实NAC后呈弥散状退缩模式者，化疗反应评价均为1级，且肿瘤范围未缩小。因此，MRI预测该病理模式的准确度、灵敏度和特异度较高，NAC后退缩呈该模式的患者不适合行BCT。目前认为，NAC后MRI显示肿瘤退缩成孤立状的患者更适合行保乳手术[21]。然而，本研究发现MRI预测孤立状模式的特异度和阳性预测值均最低，原因可能为NAC后肿瘤内部组织纤维化、坏死及炎性反应引起MRI图像持续强化。因此，对于NAC后MRI显示肿瘤呈孤立状退缩模式的患者，选择行BCT时需谨慎对待。

本研究通过MRI与病理检查比较发现，两者评价临床-病理退缩模式具有显著的一致性。同时，MRI预测临床-病理退缩模式的ROC下面积为0.928，故可认为MRI预测临床-病理退缩模式准确度高，能够指导NAC后行保乳手术者的筛选。

NAC后MRI三维重建图像能准确模拟并预测残余肿瘤的立体空间位置，有助于选择NAC后降期保乳患者。乳腺次连续病理大切片制作和MRI、病理三维重建提供了一种全新的残余肿瘤评价方法，为该领域的研究提供了崭新的平台。

[参 考 文 献]

[1] KAUFMANN M, HORTOBAGYI G N, GOLDHIRSCH A, et al. Recommendations from an international expert panel on the use of neoadjuvant (primary) systemic treatment of operable breast cancer: an update [J]. J Clin Oncol, 2006, 24(12): 1940-1949.

[2] KAUFMANN M, VON MINCKWITZ G, BEAR H D, et al. Recommendations from an international expert panel on the use of neoadjuvant (primary) systemic treatment of operable breast cancer: new perspectives 2006 [J]. Ann Oncol, 2007, 18(12): 1927-1934.

[3] CAUDLE A S, HUNT K K. The neoadjuvant approach in breast cancer treatment: it is not just about chemotherapy anymore [J]. Curr Opin Obstet Gynecol, 2011, 23(1): 31-36.

[4] KAUFMANN M, VON MINCKWITZ G, MAMOUNAS E P, et al. Recommendations from an international consensus conference on the current status and future of neoadjuvant systemic therapy in primary breast cancer [J]. Ann Surg Oncol, 2012, 19(5): 1508-1516.

[5] ISHITOBI M, OHSUMI S, INAJI H, et al. Ipsilateral breast tumor recurrence(IBTR) in patients with operable breast cancer who undergo breast-conserving treatment after receiving neoadjuvant chemotherapy: risk factors of IBTR and validation of the MD Anderson Prognostic Index [J]. Cancer, 2012, 118(18): 4385-4393.

[6] CHEN A M, MERIC-BERNSTAM F, HUNT K K, et al. Breast conservation after neoadjuvant chemotherapy: the MD Anderson cancer center experience [J]. J Clin Oncol, 2004, 22(12): 2303-2312.

[7] RASTOGI P, ANDERSON S J, BEAR H D, et al. Preoperative chemotherapy: updates of National Surgical Adjuvant Breast and Bowel Project Protocols B-18 and B-27 [J]. J Clin Oncol, 2008, 26(5): 778-785.

[8] VAN DER HAGE J A, VAN DE VELDE C J, JULIEN J P, et al. Preoperative chemotherapy in primary operable breast cancer: results from the European Organization for Research and Treatment of Cancer trial 10902 [J]. J Clin Oncol, 2001, 19(22): 4224-4237

[9] ROSEN E L, BLACKWELL K L, BAKER J A, et al. Accuracy of MRI in the detection of residual breast cancer after neoadjuvant chemotherapy [J]. AJR Am J Roentgenol, 2003, 181(5): 1275-1282.

[10] BHATTACHARYYA M, RYAN D, CARPENTER R, et al. Using MRI to plan breast-conserving surgery following neoadjuvant chemotherapy for early breast cancer [J]. Br J Cancer, 2008, 98(2): 289-293.

[11] AKAZAWA K, TAMAKI Y, TAGUCHI T, et al. Preoperative evaluation of residual tumor extent by three-dimensional magnetic resonance imaging in breast cancer patients treated with neoadjuvant chemotherapy [J]. Breast J, 2006, 12(2): 130-137.

[12] KIM H J, IM Y H, HAN B K, et al. Accuracy of MRI for estimating residual tumor size after neoadjuvant chemotherapy in locally advanced breast cancer: relation to response patterns on MRI [J]. Acta Oncol, 2007, 46(7): 996-1003.

[13] YEH E, SLANETZ P, KOPANS D B, et al. Prospective comparison of mammography, sonography, and MRI in patients undergoing neoadjuvant chemotherapy for palpable breast cancer [J]. AJR Am J Roentgenol, 2005, 184(3): 868-877.

[14] MARINOIVCH M L, HOUSSAMI N, MACASKILL P, et al. Meta-analysis of magnetic resonance imaging in detecting residual breast cancer after neoadjuvant therapy [J]. J Natl Cancer Inst, 2013, 105(5): 321-333.

[15] LOBBES M B, PREVOS R, SMIDT M, et al. The role of

magnetic resonance imaging in assessing residual disease and pathologic complete response in breast cancer patients receiving neoadjuvant chemotherapy: a systematic review [J]. Insights Imaging, 2013, 4(2): 163–175.

[16] LONDERO V, BAZZOCCHI M, DEL FRATE C, et al. Locally advanced breast cancer: comparison of mammography, sonography and MR imaging in evaluation of residual disease in women receiving neoadjuvant chemotherapy [J]. Eur Radiol, 2004, 14(8): 1371–1379.

[17] MORROW M, WATERS J, MORRIS E. MRI for breast cancer screening, diagnosis, and treatment [J]. Lancet, 2011, 378(9805): 1804–1811.

[18] BAHRI S, CHEN J H, MEHTA R S, et al. Residual breast cancer diagnosed by MRI in patients receiving neoadjuvant chemotherapy with and without bevacizumab [J]. Ann Surg Oncol, 2009, 16(6): 1619–1628.

[19] DE LOS SANTOS J F, CANTOR A, AMOS K D, et al. Magnetic resonance imaging as a predictor of pathologic response in patients treated with neoadjuvant systemic treatment for operable breast cancer. Translational Breast Cancer Research Consortium trial 017 [J]. Cancer, 2013, 119(10): 1776–1783.

[20] WASSER K, SINN H P, FINK C, et al. Accuracy of tumor size measurement in breast cancer using MRI is influenced by histological regression induced by neoadjuvant chemotherapy [J]. Eur Radiol, 2003, 13(6): 1213–1223.

[21] THIBAULT F, NOS C, MEUNIER M, et al. MRI for surgical planning in patients with breast cancer who undergo preoperative chemotherapy [J]. AJR Am J Roentgenol, 2004, 183(4): 1159–1168.

（收稿日期：2014–08–07 修回日期：2015–03–08）